# Effect of global warming on Indian monsoon simulated with a coupled ocean-atmosphere general circulation model

**M. Lal*, U. Cubasch and B. D. Santer****

Deutsches Klimarechenzentrum GmbH, D-2000 Hamburg 13, Germany

* Visiting scientist. Permanent affiliation is with the Centre for Atmospheric Sciences, Indian Institute of Technology, New Delhi 110 016, India

** Present address: Lawrence Livermore National Laboratory, Livermore, CA 94550, USA

**The impact of increasing greenhouse gas concentrations on the climate of Indian subcontinent and its variability is studied using the output from a time-dependent greenhouse warming simulation as well as a reference control experiment performed with the Hamburg global coupled atmosphere-ocean circulation model. This model demonstrates substantial skill in simulating the present-day climate and its inter-annual variability over the monsoon region. The onset date of the SW-monsoon over India along about 20°N inferred from the control run is similar to the observed onset date. With the exception of temperature, the projected changes in impact-related climatic variables over a period of 100 years are within the range of inter-annual variability in the monsoon region. There is no clear evidence for a significant change in the seasonal-mean monsoon rainfall or the variability of the monsoon rainfall in scenario A experiment.**

IN the tropics, the amplitude of the annual cycle in surface temperatures is far greater over land than over the oceans. This results in seasonal reversal of the land-ocean temperature difference that drives the regional monsoon circulation. While the rainy season is short and unreliable along the western semi-arid margins of the Indian subcontinent, monsoon depressions forming over the Bay of Bengal travel in a northwesterly to northerly direction and lead to recurrent flooding in Bangladesh and the adjoining eastern hilly regions of India. Above or below normal monsoon rainfall over the Indian subcontinent may be catastrophic or beneficial depending on its timing, location and intensity.

The current paper assesses the possible impacts of a potential change on the monsoon climate by future increases in anthropogenic greenhouse gases. Previous GCM-related studies of the climate change in the monsoon region are based on numerical experiments conducted with the atmospheric models[1-3] or with atmospheric models coupled to a simple mixed layer ocean[4-8]. These simulations describe the equilibrium response of the models to instantaneous doubling of $CO_2$. More recent GCMs treat the coupled atmosphere-ocean system in an interactive mode and are able to provide projections of the possible perturbations in key climatic elements in the time scales of up to 100 years[9-11].

Apart from a reference control experiment, a time-dependent greenhouse warming simulation has recently been carried out at the Max-Planck-Institute for Meteorology (MPIM), Hamburg using a coupled global ocean-atmosphere circulation model and greenhouse gas change scenario A ('*business as usual*' in which future emissions of greenhouse gases are allowed to increase unrestricted).

Prior to assessing the climate change due to greenhouse forcing, it is important to determine how well the model simulates the present-day climate over the region of interest. The output available from the reference control experiment has been analysed to validate the performance on the model for the Asian monsoon region the findings of which are presented first. A plausible future monsoon climate scenario for the region based on numerical results obtained from greenhouse warming simulation for scenario A is discussed as well.

## The coupled climate model

The atmospheric component (ECHAM1) of the Hamburg climate model evolved from a low horizontal resolution (T21: triangular spectral cutoff at wave number 21) numerical weather forecasting model of *E*uropean *C*entre for Medium Range Weather Forecasts, UK[12] and has undergone extensive modifications at *Ham*burg for its climate applications[13]. The prognostic variables are vorticity and divergence, temperature, surface pressure, water vapour and cloud water (droplets and crystals). The introduction of cloud water as an additional prognostic variable enables a more realistic simulation of clouds, precipitation and radiation. The

diurnal cycle is included. Sub-grid scale physical processes parameterized in the model include radiation, cloud formation, precipitation, turbulent mixing and convection. The runoff into the ocean is calculated using a simple surface hydrology model[14].

The spectral representation is transformed to a 5.6° Gaussian grid to calculate the nonlinear advection terms and physical processes. Vertically, the model is discretized on 19 levels in a hybrid $\sigma$-$p$ system. The semi-implicit integration scheme (leapfrog with time filter) uses a time step of 40 minutes. The surface boundary conditions include the blended data sets for sea surface temperature and sea ice thickness[15, 16] and the orography is based on mean terrain heights computed from high resolution US Navy data sets.

The ocean component (LSG) of the model is based on a numerical formulation of the primitive equations[17] appropriate for *l*arge *s*cale *g*eostrophic motion. The nonlinear advection of momentum is neglected and fast gravity waves are strongly damped by an implicit time integration scheme using a time step of 30 days. The salinity and temperature transport through currents is computed with an upstream advection scheme. A small explicit horizontal diffusion of 200 $m^2$ is introduced to counteract the inherent tendency for mode-splitting in the E-grid used in the horizontal discretization scheme. Vertical convective mixing is applied whenever the stratification becomes unstable. Sea ice is computed from the ice heat balance and the advection by oceanic currents, using a simplified viscous rheology. A realistic bottom topography is included.

The discretization of the ocean model is based on 11 unequally-spaced vertical levels and two overlapping $5.6° \times 5.6°$ horizontal grids (corresponding to an effective net grid size of 4°) which are interpolated onto the resolution of the Gaussian grid used in ECHAM1. In the coupled mode, the basic time step of 30 days is reduced to 1 day for the computation of sea ice and the temperature and salinity in the two uppermost ocean layers in order to resolve the rapid response of the upper ocean to the short-term variability of the atmosphere.

The ECHAM1 and LSG are coupled by the air-sea fluxes of momentum, sensible and latent heat, short and long wave radiation and fresh water (evaporation – precipitation + runoff along the coastal boundaries). To avoid a climate drift of the coupled system in long-time integrations, a flux correction is applied[18]. Both the models are integrated synchronously, but with their respective time steps. The fluxes computed at each 40-minute time step of the ECHAM1 are summed up over one full time step of LSG and are then transferred to the uppermost layer of the ocean model.

The control reference atmosphere has been simulated with the coupled climate model over a 100-year period from 1985 to 2084 with constant 1985 atmospheric $CO_2$ concentration. The model simulates the general structure of the mean atmospheric circulation reasonably well. In the ocean, the control run reproduces the observed salinity and temperature fields and is consistent with the conveyer belt picture of the global ocean circulation. In scenario A (*business as usual*) experiment, the net radiative forcing of all greenhouse gases is represented in terms of equivalent $CO_2$ concentration (1.2% per year compound increase of $CO_2$). The global average near-surface temperature increase of 2.6 K in scenario A at the end of the simulation lies close to the IPCC's best estimate[19]. However, the global average temperature change in years 10–50 of scenario A experiment is consistently lower than the IPCC estimates possibly due to the strong oceanic heat uptake resulting from a more realistic description of the deep ocean in the model. For further details on the description of the model and its performance in simulating the general features of the mean atmospheric and oceanic circulations on global as well as temporal scales, the reader is referred to Cubasch *et al.*[11].

## Results

The monsoon region selected for our study is bounded by latitudes 2.8°S to 36.6°N and longitudes 61.7°E to 101.0°E (Indian subcontinent and adjoining seas). In a recent study on statistical strategy to deduce regional scale features from general circulation models, Storch *et al.*[20] concluded that the Hamburg climate model results could be questionable for spatial scales smaller than 4 grid points. Our study area, however, has a total of 64 grid points ($8 \times 8$) and the application of the model output to the selected region should yield meaningful inferences. For validation of the present-day climate over the region, we have analysed the data from control experiment for all the four seasons, namely, winter (December to February), pre-monsoon (March to May), monsoon (June to September) and post-monsoon (October to November). To assess the climate change, however, the data analysed and presented here relate only to the monsoon season. This season is regarded as most vital for the region as over 70% of the total annual rainfall occurs during June to September in association with the SW-monsoon.

## Regional scale model climate: the control experiment

In a previous study, it has been shown that the atmospheric component of the Hamburg climate model is capable of simulating the monthly mean meteorological parameters associated with the monsoon with some skill[21]. In the coupled climate model (ECHAM1 + LSG), the seasonal mean surface pressure, wind and

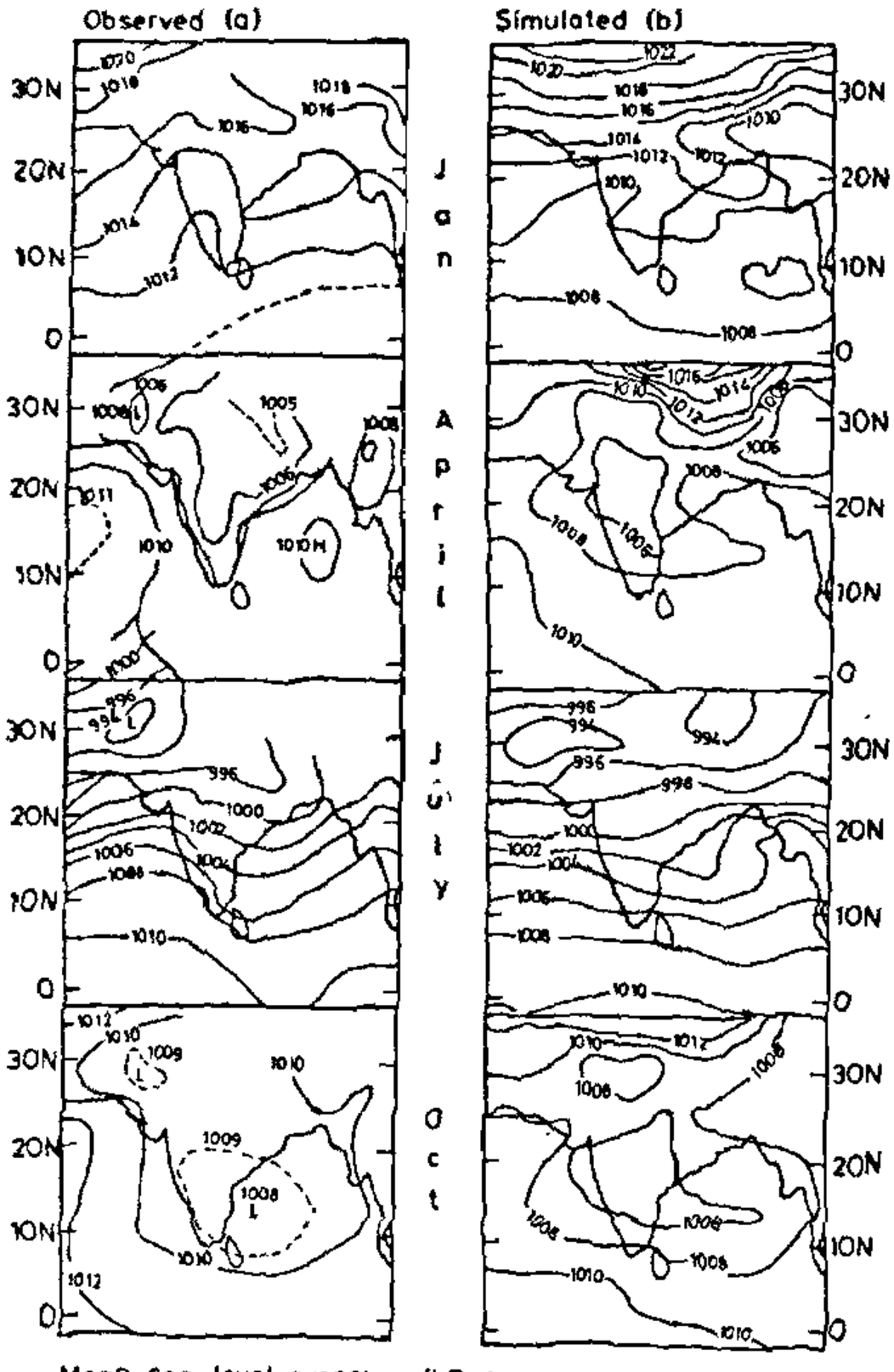


Figure 1. Seasonal variation in mean sea level pressure (hPa) as (*a*) observed (source: Rao[22]) and (*b*) simulated by the climate model (control experiment) over the study area.

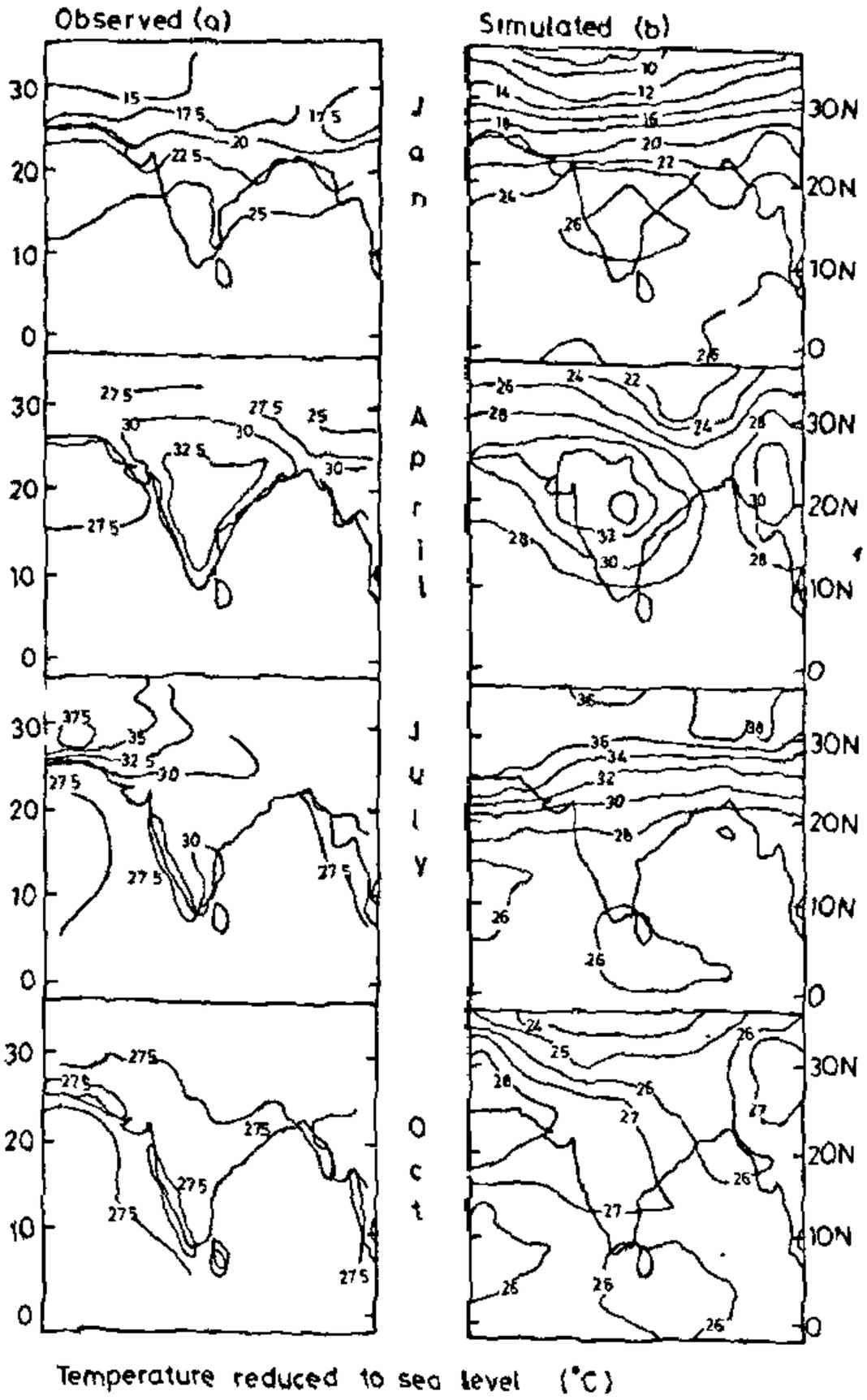


Figure 2. Seasonal variation in surface air temperature (in °C as *reduced to mean sea level*) as (*a*) observed (source. Rao[22]) and (*b*) simulated by the climate model (control experiment) over the study area

precipitation distributions over the selected region as inferred from the average of the first ten years of control run exhibit similarity to the observed patterns. The model-simulated mean patterns of surface pressure, temperature, wind and precipitation for the four months namely, January, April, July and October representing winter, pre-monsoon, monsoon and post-monsoon seasons respectively over the region have been analysed.

The seasonal changes in spatial pattern of mean sea level pressure (Figure 1) illustrate the simulation of an elongated zone of low pressure along the Indo-Gangetic plains of north India during July. As is evident from both model-simulated and observed surface pressure fields, the axis of this low pressure area (known as 'monsoon trough') is roughly oriented from northwest to southeast. The high pressure over the Tibetan Plateau in January and low pressure over the northwest India in July are realistically simulated by the model[22].

The seasonal changes in 2 m temperature (Figure 2) are simulated by the model quite satisfactorily as compared with those observed over the region[20]. The semi-arid region of northwest India is an area of high surface temperature during July which gradually builds up in the pre-monsoon season. The geographic location of the thermal high coincides fairly well with the position of the area of low surface pressure in the model simulation.

One of the most dramatic examples associated with summer monsoon over India is the reversal of the wind flow over south India from north-easterly during January to south-westerly during July. This feature has been distinctly observed in the model-simulated surface wind field. The depth of monsoon current off the west coast of India is from surface to about 600 hPa in the model-simulated wind field during July.

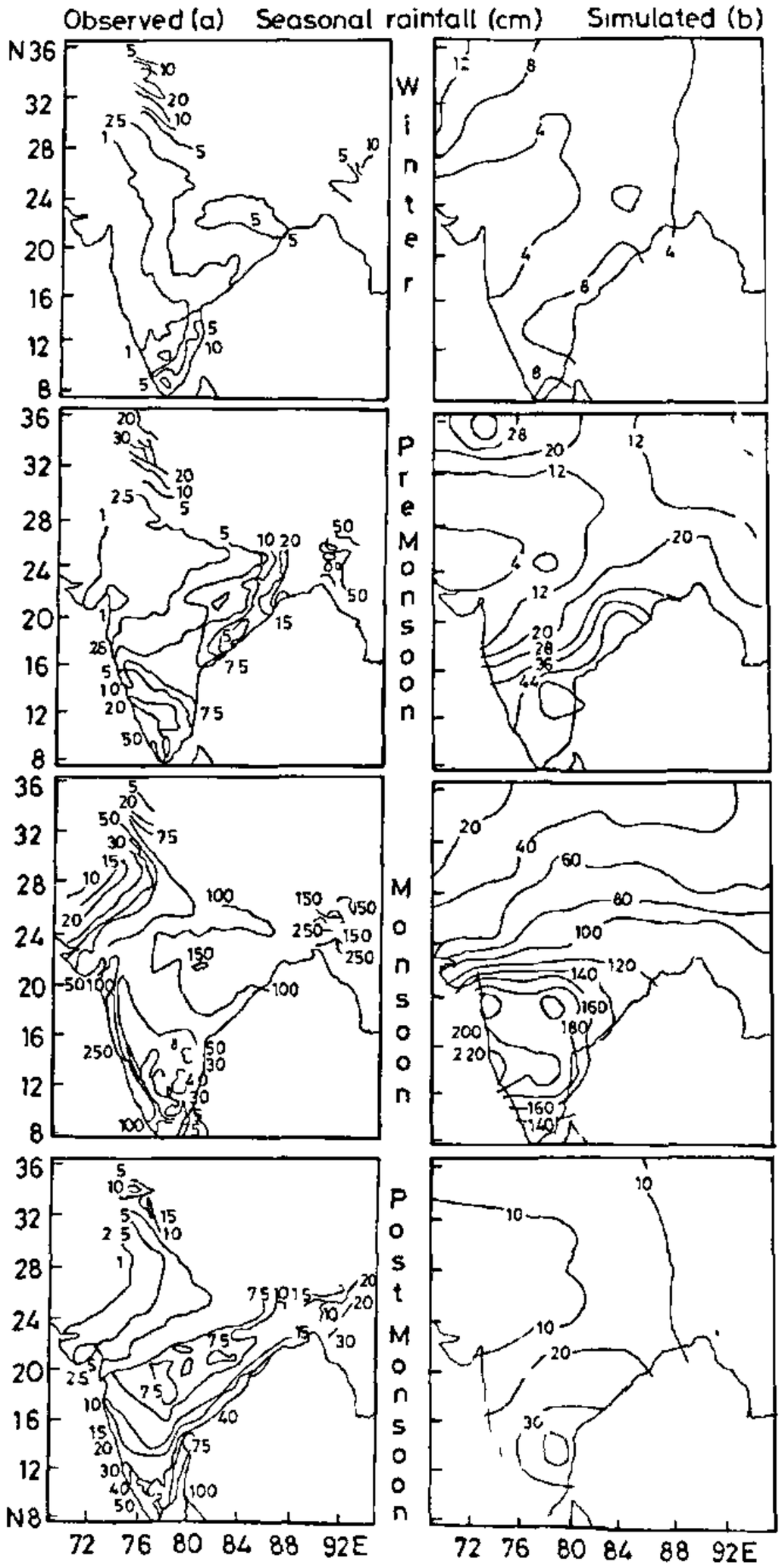


Figure 3. Distribution of seasonal rainfall (cm) over the study area during the winter, pre-monsoon, monsoon and post-monsoon seasons as (*a*) observed (source Rao[22]) and (*b*) simulated by the climate model

Of the annual rainfall simulated by the model over the study area, almost 78% is found to occur during the months June–September. Winter is, as observed[22], drier over most parts of the subcontinent in the model-simulated precipitation distribution (Figure 3). Rainfall is, however, observed in the model simulation over the southern tip of India under the influence of NE-monsoon. Over the northern extremes of the Indian subcontinent, rainfall also occurs in association with the frontal systems of mid-latitude westerlies. During pre-monsoon months, enhanced convective activity over the peninsular India and associated precipitation are simulated well by the model (Figure 3). The model-simulated total rainfall during monsoon as averaged for the land points over the study area (102.3 cm) is close to the climatological seasonal total rainfall (88 cm) over India. The model is, however, not able to reproduce the spatial variability of rainfall over northwest India and the sharp gradient from west to east coast over the south peninsula. This could possibly be attributed to the coarse resolution of the model.

The model captures the characteristic features of the vertical distribution of temperature, specific humidity and winds as observed[22, 23] over the region. There is evidence of the formation of a heat low (an elevated heat source) and an anticyclone over Tibet at elevations around 500 hPa and 200 hPa respectively during the pre-monsoon season in model-simulated vertical thermal structure. Figure 4 depicts the observed and model-simulated distributions of specific humidity at 850 hPa level during winter and monsoon seasons. During the monsoon season, the model simulation produces a deep (extending from surface to above 500 hPa level) moist air only to the east of 60°E over the south Arabian Sea. This build-up of moist air over the south Arabian Sea has a powerful impact on the characteristics of the southwest monsoon flow over India.

The location and strength of the tropical easterly jet over the Indian subcontinent, which is a typical upper-air circulation feature associated with the Asian summer monsoon, simulated by the model coincides with observed climatology (Figure 5; Rao[22]). This easterly jet, so well marked at 100 hPa level over the region during monsoon season, disappears during winter (during pre-monsoon season, the easterly winds have as yet not attained the core speed of 60 kts or more and are located south over the Indian Ocean) while the sub-tropical westerly jet (with maximum core speed at 200 hPa level) located at northern limits of the region strengthens and shifts further south over north India in the model-simulated upper-air wind field.

The inter-annual variability in the surface temperature and precipitation over the study area has been examined in the data from 100 years of control run. The range of seasonal temperature anomalies (–0.59 K to 0.61 K) simulated by the model (year-to-year deviation from the 100-year mean seasonal temperature averaged for all land points) is close to the observed[24, 25] range (–0.79 K to 0.60 K) in the mean seasonal temperature anomaly data for the period 1901–1981 (Figure 6*a*). An F-test indicates that the difference in variances of the two time series of temperature anomalies is not significant at 1% level. The observed[26, 27] extreme events in the seasonal mean rainfall anomalies (±28 cm) are almost higher by a factor of two (Figure 6*b*) than those in the model simulation (±15 cm).

**Table 1.** Difference in area-averaged hydrological parameters (5°N–35°N and 65°E–100°E, land points only) of weak and strong monsoon years for control and scenario A simulations each for 60 years duration ($CO_2$ doubling time in scenario A) with the Hamburg (ECHAM1 + LSG) climate model

| | Control | | | Scenario-A |
|---|---|---|---|---|
| Elements | Weak | Strong | Difference | Difference |
| 2 m temperature (C) | 20 43 | 20 02 | + 0 41 | + 0 64 |
| Precipitation (mm/day) | 7 63 | 9 40 | − 1 77 | − 1 87 |
| Evaporation (mm/day) | 2 27 | 2 41 | − 0 14 | − 0 09 |
| Soil moisture (cm) | 11 69 | 12 50 | − 0 81 | − 1 02 |
| Conv precipitation (mm/day) | 5 87 | 7 39 | − 1 52 | − 1.36 |
| Cloud cover (%) | 63 38 | 68 15 | − 4 77 | − 5 57 |

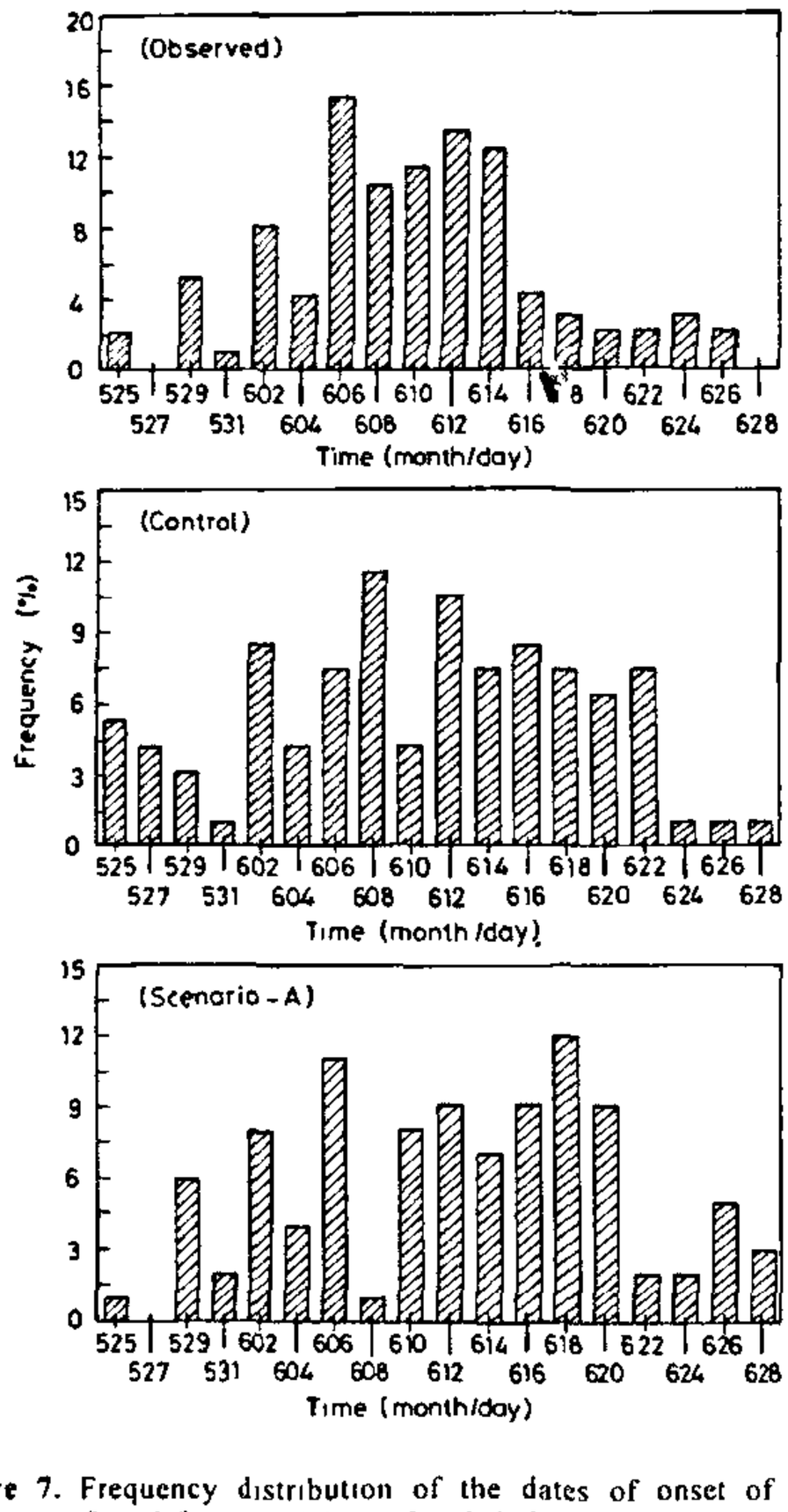


**Figure 7.** Frequency distribution of the dates of onset of SW-monsoon inferred from model-simulated daily rainfall data at three land grid points along 19 67°N in the control run and scenario A experiment (years 1–100) and the dates of onset actually recorded at Bombay (19°N, period 1879–1975)

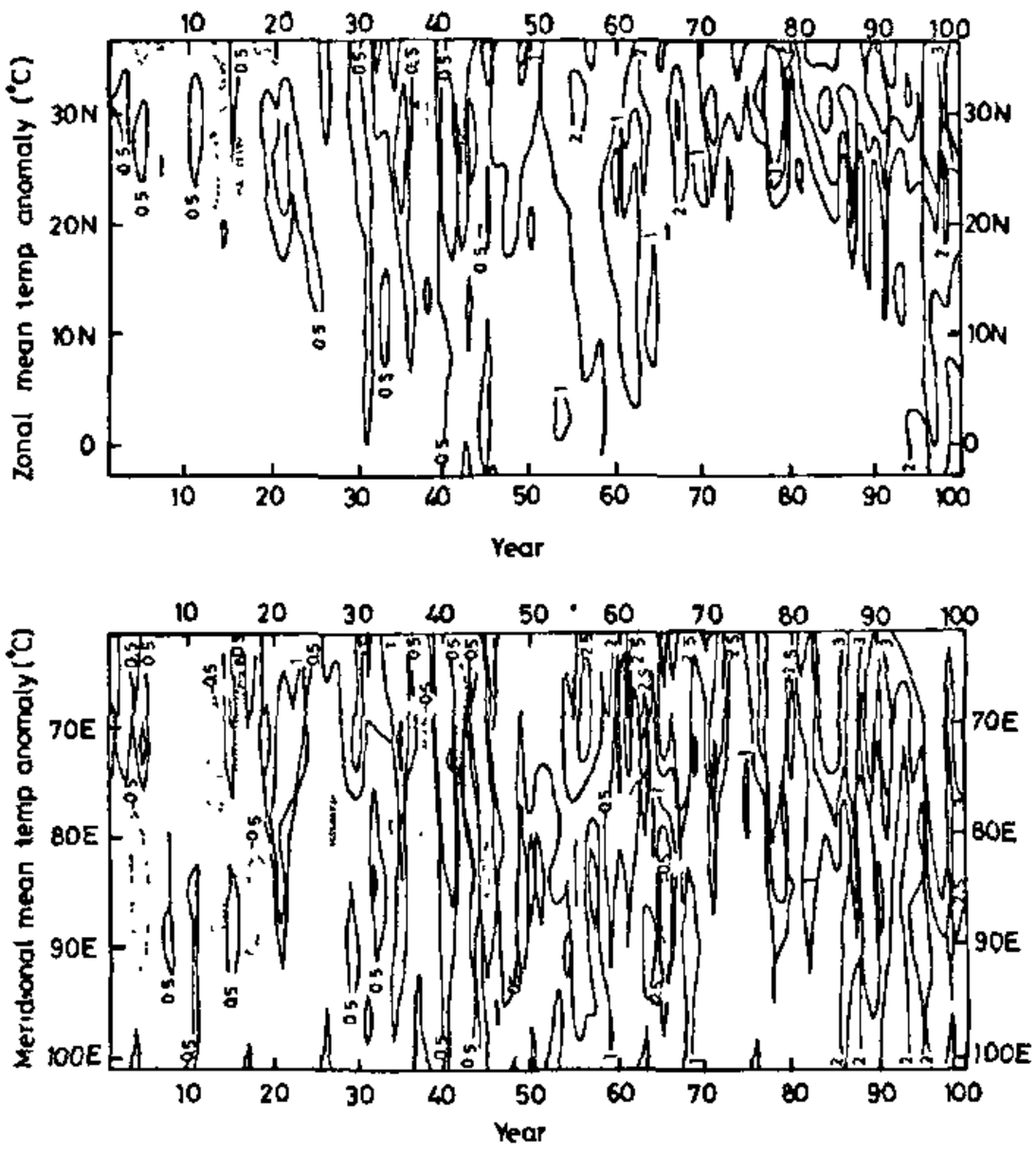


**Figure 8.** Time evolution of the model-simulated zonal (all grid points) and meridional (land points only) mean distributions of change in surface air temperature over the study area under scenario A conditions

no evidence of a signal in soil moisture, a distinct, although weak, signal in evaporation is observed.

An analysis of daily rainfall data for 100 years of scenario A integration using the monsoon onset criterion above indicates a mean monsoon onset date of 11 June. Even, if only the last 50 years of scenario A simulation are considered, the mean onset date shifts only to the 12th June. A comparison of the frequency distributions of the onset dates derived for control and scenario A experiments with those observed at Bombay (19°N) is illustrated in Figure 7. A *t*-test and *F*-test on the observed onset dates and those inferred from the control run and scenario A experiment indicated that the onset dates derived from scenario A experiment do not exhibit any evidence for a significant change in the mean onset date or in the inter-annual variability of the onset date.

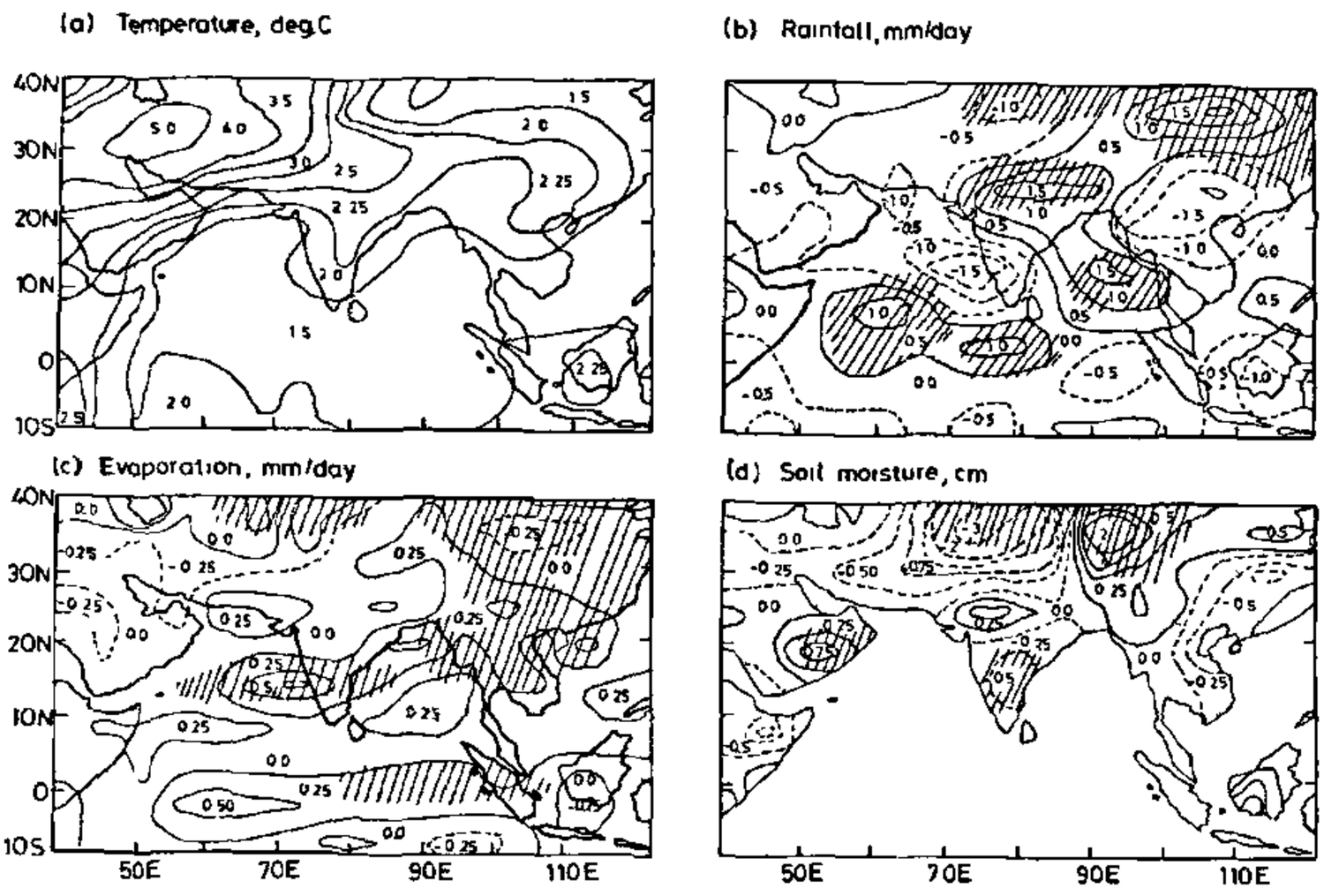


**Figure 9** Spatial distribution of the model-simulated changes in (*a*) temperature, (*b*) rainfall, (*c*) evaporation, and (*d*) soil moisture over the study area [last decade of scenario A relative to first decade of control run, the hatched areas in (*b*), (*c*) and (*d*) represent the significant changes at 90% level].

To examine the inter-annual variability in seasonal rainfall over India, the area-averaged monsoon rainfall over the region more (less) than plus (minus) one standard deviation are identified as strong (weak) monsoons in the 60 year's data ($CO_2$ doubling time) of control and scenario A simulations. While a substantial difference in the rainfall is observed between strong and weak monsoon cases, no significant changes are found in the rainfall variability between weak and strong monsoons in enhanced $CO_2$ simulation with respect to those in the control experiment. The other hydrological parameters also do not indicate any enhanced inter-annual variability over India (Table 1) in a warmer atmosphere.

The zonal (all grid points) and meridional (land points only) mean time-evolution of temperature anomalies over the selected region as simulated by the model (scenario A) provide further information on the projected spatial and temporal variations in temperature rise expected over the Indian subcontinent associated with the global warming. A distinct contrast in both north-south (in zonal means) and east-west (in meridional means) distribution of temperature increase is observed over the region (Figure 8). The impact of greenhouse warming is far greater over land than over the oceans, a feature similar to those reported for other regions in coupled model simulations[10, 11, 28]. In scenario A experiment, the maximum warming of about 2.5 K to 3.0 K is between 20°N and 35°N and most pronounced in the region bounded by 60°E and 80°E meridians (semi-arid regions of northwest India).

The spatial distribution of change in temperature, precipitation, evaporation and soil moisture in the final decade of the scenario A experiment relative to the mean of the first decade of the control run is given in Figure 9. This suggests that, while most of the Indian subcontinent warms (statistically significant at 95% level) by over 2 K over the next 100 years, the warming is most pronounced over the north-western margins of India. While less precipitation could occur over the southern peninsular India (statistically significant at 90% level), an enhanced precipitation largely confined over the central plains of India is simulated by the model. The evaporation rate over most of the subcontinent also increases (significant at 90% level only over south peninsular India) as a result of surface temperature rise. A depletion in soil moisture over the south peninsula and along the semi-arid regions of NW-India (statistically significant at 90% level for both the locations) is simulated.

## Conclusions

The Hamburg coupled climate model demonstrates substantial skill in simulating the present-day climate and its inter-annual variability over the monsoon region The results obtained from the greenhouse warming experiment suggest that the surface temperature could significantly change by ≥2 K over the monsoon region in the next 100 years. For other relevant climatic variables, significant climatic changes could only be

isolated over some areas. There is no evidence for a significant change in the mean monsoon rainfall or in its inter-annual variability. It may be stressed here that the present study is only one realization. Additional model simulations with different initial conditions and further experiments with a finer resolution model having more realistic convective parametrization in the tropics are desired to focus on these details.


1 Washington, W. M. and Daggupaty, S M., *Mon. Weather Rev*, 1975, **103**, 105–114.
2 Shukla, J , *J Atmos. Sci.*, 1975, **32**, 503–511
3 Druyan, L. M , *J. Climatol*, 1982, **2**, 127–139.
4 Washington, W. M. and Meehl, G. A., *J Geophys Res*, 1984, **89**, 9475–9503.
5. Meehl, G A , *Mon Weather Rev.*, 1987, **115**, 27–50.
6 Kitoh, A and Tokioka, T , *J. Meteor Soc. Jpn.*, 1987, **65**, 167–187
7 Zeng, Qing-cun *et al*, *Chinese J. Atmos. Sci.*, 1988, Special Issue
8 Zhao, Z -C. and Kellogg, W W , *J. Climate*, 1988, **1**, 348–378
9 Houghton, D. D , Gallimore, R G and Keller, L. M , *J Climate*, 1991, **4**, 555–577.
10 Manabe, S , Spelman, M J and Stouffer, F J., *J Climate*, 1992, **5**, 105–126
11 Cubasch, U., Hasselmann, K., Hock, H., Maier-Reimer, E., Mikolajewicz, U., Santer, B D and Sausen, R , *Clim. Dyn*, 1992, **8**, 55–69
12. Louis, J. F (ed ), *Meteorol. Bull*, ECMWF, Shinfield Park, Reading, UK, 1986.
13. Roeckner, E. *et al.*, The Hamburg version of the ECMWF model (ECHAM), GARP Report 13, WMO, Geneva, WMO/TP-332, 1989.
14 Dumenil, L. and Todini, E , in *Advances in Theoretical Hydrology* (ed O'Kane, J. P ), European Geophysical Society Series on Hydrological Sciences, 1992, vol 1, pp 129–157.
15 Reynolds, R. W., *J Climate*, 1988, **1**, 75–86
16. Alexander, R C. and Mobley, R. L., *Mon Weather Rev*, 1974, **104**, 143–148
17. Maier-Reimer, E., Mikolojewicz, U. and Hasselmann, K., *J Phys Oceanogr*, 1992, **22**, 951–962.
18 Sausen, R., Barthel, K. and Hasselmann, K., *Clim Dyn*, 1988, **2**, 154–163.
19 Intergovernmental Panel on Climate Change 1990, Scientific assessment of climate change, WMO/UNEP Rep., (eds. Houghton, *J T. et al*), *Cambridge University Press, pp 365*
20. Storch, H. von, Zorita, E. and Cubasch, U , Downscaling of global climate change estimates to regional scales: An application to Iberian rainfall in wintertime, MPI Report No. 64, 1991, pp. 36
21. Barnett, T. P., Dumenil, L., Schlese, U., Roeckner, E. and Latif, M., *J. Atmos Sci*, 1989, **46**, 661–685
22. Rao, Y. P., Meteorol Monograph: Synoptic Meteorology No 1/1976, India Meteorol. Dept , New Delhi, 1976.
23. Oort, A H , Global atmospheric circulation statistics, 1958–1973, NOAA Prof. Paper 14, US Dept. of Commerce, Washington, DC, 1983.
24. Hingane, L. S , Rupa Kumar, K. and Ramanamurty, Bh V., *J. Climatol.*, 1985, **5**, 521–528
25. Sarkar, R P. and Thapliyal, V., *Mausam*, 1988, **39**, 127–138.
26 Mooley, D A and Parthasarathy, B., *Clim Change*, 1984, **6**, 287–301
27. Shukla, J , in *Monsoons* (eds Fein, J. S and Stephens, P. L ), Wiley, New York, 1987, pp. 399–464.
28. Intergovernmental Panel on Climate Change 1992, Climate Change: The supplementary report to the IPCC scientific assessment, WMO/UNEP Rep., (eds. Houghton, J. T , Callander, B A and Varney, S K ), Cambridge University Press, pp 200


ACKNOWLEDGEMENTS. The Max-Planck Institute for Meteorology provided stimulating hospitality to the first author (ML) during which time this research was conducted.

Received 28 June 1993, revised accepted 10 January 1994